Supplementary Information – First-principles study on structural and electrochemical properties of $Na_xTi_2O_4$ ($0 \leq x \leq 1$) with tunnel structure for anode application of alkali-ion battery

Song-Hyok Choe[1,2*], Chol-Jun Yu[1†], Yong-Chol Pak[1], Ye-Gyong Choe[1], Kwang-Il Jon[3], Jin-Song Kim[1], and Kum-Chol Ri[1]

[1]*Computational Materials Design, Faculty of Materials Science, Kim Il Sung University, Pyongyang, PO Box 76, Democratic People's Republic of Korea*

[2]*Natural Science Center, Kim Il Sung University, Pyongyang, PO Box 76, Democratic People's Republic of Korea*

[3]*Institute of Applied Physics, Faculty of Physics, Kim Il Sung University, Pyongyang, PO Box 76, Democratic People's Republic of Korea*

Crystal Structure

Table S1. The experimentally determined atomic sites, cooridnates (x, y, z) and site occupancies (Occ.) of $Na_{0.558}Ti_2O_4$ (NTO-single) and $Na_{0.5}Ti_2O_4$ (NTO-double) from Ref.[a] and Ref.[b], respectively. Both compounds crystallize in orthohombic system with a space group *pnam*.

$Na_{0.558}Ti_2O_4$[a] (NTO-single)						$Na_{0.5}Ti_2O_4$[b] (NTO-double)					
Atoom	Site	X	Y	Z	Occ.	Atoom	Site	X	Y	Z	Occ.
						Na	4c	0.6048(10)	0.25	0.0803(11)	0.33(1)
Na	4c	0.3459(3)	0.25	0.2431(4)	0.558	Na	4c	0.0752(13)	0.25	0.4103(18)	0.17(1)
Ti	4c	0.11370(7)	0.25	0.06032(9)	1.0	Ti	4c	0.83690(8)	0.25	0.25850(9)	1.0
Ti	4c	0.60279(7)	0.25	0.08417(8)	1.0	Ti	4c	0.12408(7)	0.25	0.02124(8)	1.0
O	4c	0.6451(3)	0.25	0.2947(3)	1.0	O	4c	0.6899(3)	0.25	0.3682(4)	1.0
O	4c	0.9818(3)	0.25	0.3883(3)	1.0	O	4c	0.4044(3)	0.25	0.1500(3)	1.0
O	4c	0.2170(3)	0.25	0.4759(3)	1.0	O	4c	0.2670(3)	0.25	0.3683(3)	1.0
O	4c	0.9288(3)	0.25	0.0761(3)	1.0	O	4c	0.9573(3)	0.25	0.0995(3)	1.0

Table S2. Lattice constants (a, b, c) and unit cell volume of $Na_xTi_2O_4$ (x = 0.5, 1.0), and their relative errors to the corresponding experimental data.

	Lattice constant (Å)			Volume	Relative error (%)			
	a	b	c	(Å^3)	Δa	Δb	Δc	ΔV
	x = 0.5 (NTO-single)							
Exp.[a,*]	9.139	10.719	2.956	289.572	–	–	–	–
PBE	9.174	10.795	2.967	293.818	0.383	0.709	0.372	1.466
PBEsol	9.112	10.626	2.939	284.602	−0.295	−0.868	−0.575	−1.716
	x = 1.0 (NTO-single)							
Exp.[c]	9.262	10.754	2.956	294.361	–	–	–	–
PBE	9.347	10.835	2.948	298.568	0.918	0.753	−0.271	1.429
PBEsol	9.254	10.746	2.895	287.854	−0.086	−0.074	−2.064	−2.211
	x = 0.5 (NTO-double)							
Exp.[b]	9.616	11.134	2.954	316.279	–	–	–	–
PBE	9.673	11.230	2.967	322.315	0.593	0.862	0.440	1.908
PBEsol	9.554	11.124	2.983	311.730	−0.645	−0.090	0.982	−1.438

[a] Y. Takahashi, et al., J. Solid State Chem. 180 (2007) 1020–1027.

[*] Experiment for $Na_{0.558}Ti_2O_4$.

[b] J. Akimoto and H. Takei, J. Solid State Chem. 90 (1991) 92–101.

[c] J. Akimoto and H. Takei, J. Solid State Chem. 79 (1989) 212–217.

[*] sh.choi0220@ryongnamsan.edu.kp
[†] cj.yu@ryongnamsan.edu.kp

Structural properties

Table S3. Lattice constant (a, b, c), unit cell volume (V) and relative volume change rate ($r_{vol} = (V_x - V_{0.5})/V_{0.5} \times 100\ \%$) in $Na_xTi_2O_4$ polymorphs (NTO-single and NTO-double).

x	Lattice constant (Å)			Volume	r_{vol}
	a	b	c	(Å^3)	(%)
	NTO-single				
0.0	8.986	10.768	5.960	576.674	−1.899
1/8	9.037	10.775	5.955	579.877	−1.336
2/8	9.092	10.771	5.951	582.804	−0.827
3/8	9.144	10.786	5.940	585.830	−0.306
4/8	9.174	10.795	5.934	587.625	0.000
5/8	9.234	10.785	5.938	591.331	0.627
6/8	9.274	10.813	5.916	593.188	0.938
7/8	9.315	10.821	5.906	595.301	1.289
1.0	9.347	10.835	5.897	597.137	1.593
	NTO-double				
0.0	9.827	9.733	6.037	577.446	−11.634
1/8	9.806	10.779	5.998	633.880	−1.695
2/8	9.855	10.953	5.971	644.539	−0.014
3/8	9.760	11.115	5.953	645.781	0.179
4/8	9.673	11.230	5.934	644.627	0.000
5/8	9.674	11.257	5.935	646.301	0.259
6/8	9.630	11.288	5.936	645.305	0.105
7/8	9.503	11.325	5.948	639.942	−0.732
1.0	9.525	11.347	5.936	641.513	−0.485

The relative volume change rate (r_{vol}) is considered as an important factor showing the structural stability of electrode materials. Since the existence of $Na_xTi_2O_4$ ($x < 0.5$) is unclear, especially for $x = 0.0$, r_{vol} is calculated referring to the unit cell volume of medium Na content $x = 0.5$, which is identified experimentally for both NTO-single and NTO-double phases.

Na^+ ion migration

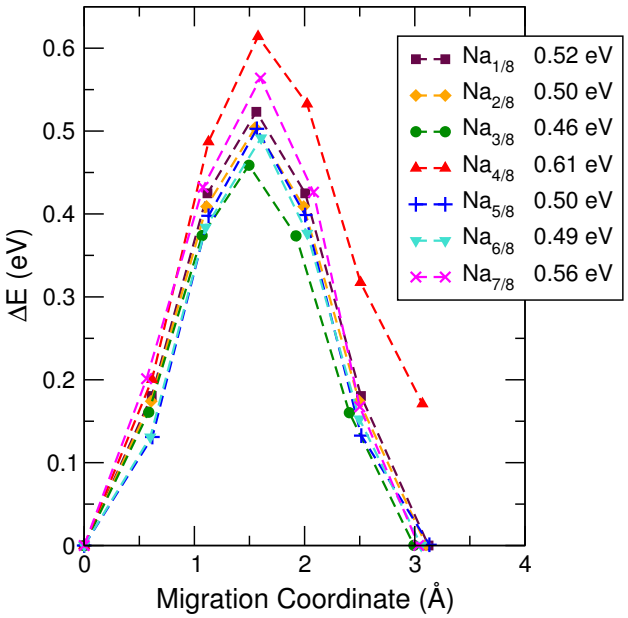

Figure S1. Energy profile caculated by NEB method for Na^+ ion migration along *c*-axis in $Na_xTi_2O_4$ of NTO-single compounds. The Na content *x* and the corresponding activation barrier for Na^+ ion migration are given in legend.

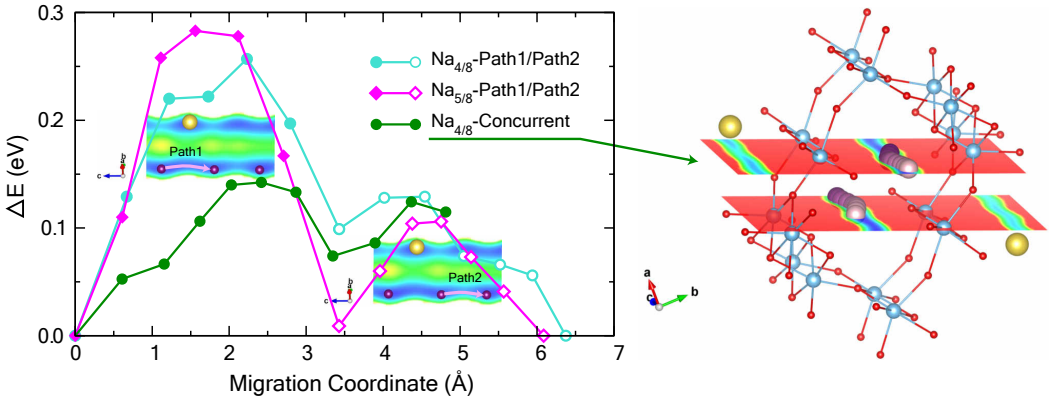

Figure S2. Energy profile calculated by NEB method for Na^+ ion migration along the *c*-axis in $Na_xTi_2O_4$ in the double phase at $x = 0.5$ and $x = 0.625$. The filled and empty shapes in the graph represent the total energy differences of the NEB images along the path1, passing by Na^+ ion at rest, and path2, respectively. The green solid lines display the energy profile of the concurrent move of two Na^+ ions inside the tunnel in $Na_{0.5}Ti_2O_4$, and the migration path is illustrated in the picture of crystal structure next to the graph, where the BVS map is also given and the balls in purple-to-pink color show the sequential locations of the two Na^+ ions during migration.

Partial density of states

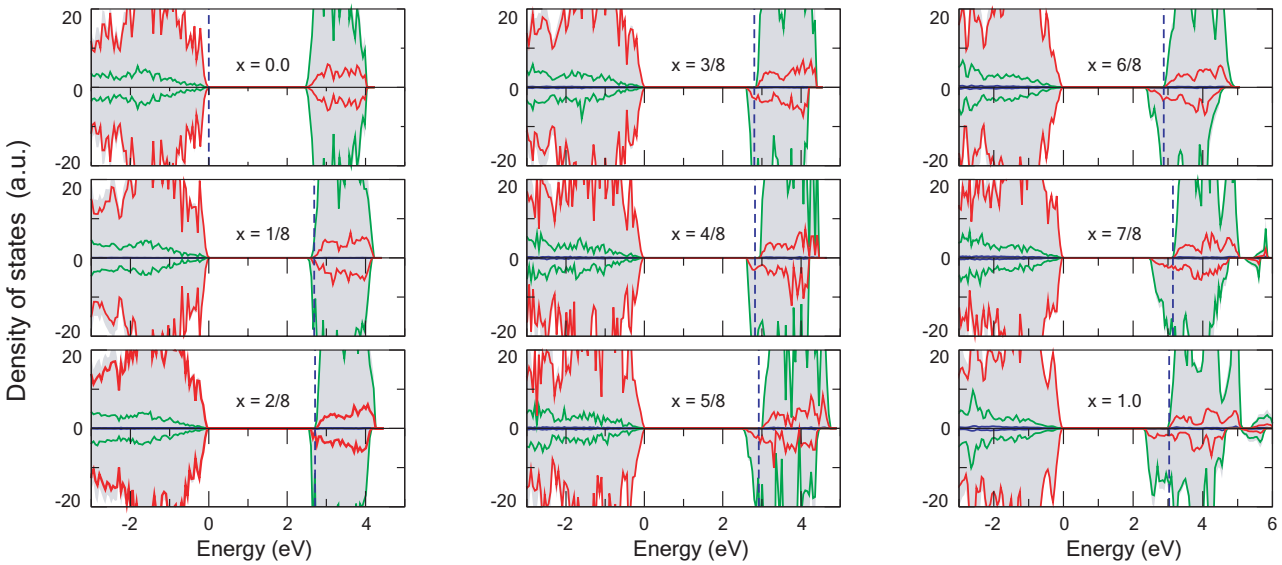

Figure S3. Atom resolved partial DOS (PDOS) of $Na_xTi_2O_4$ in the single phase.

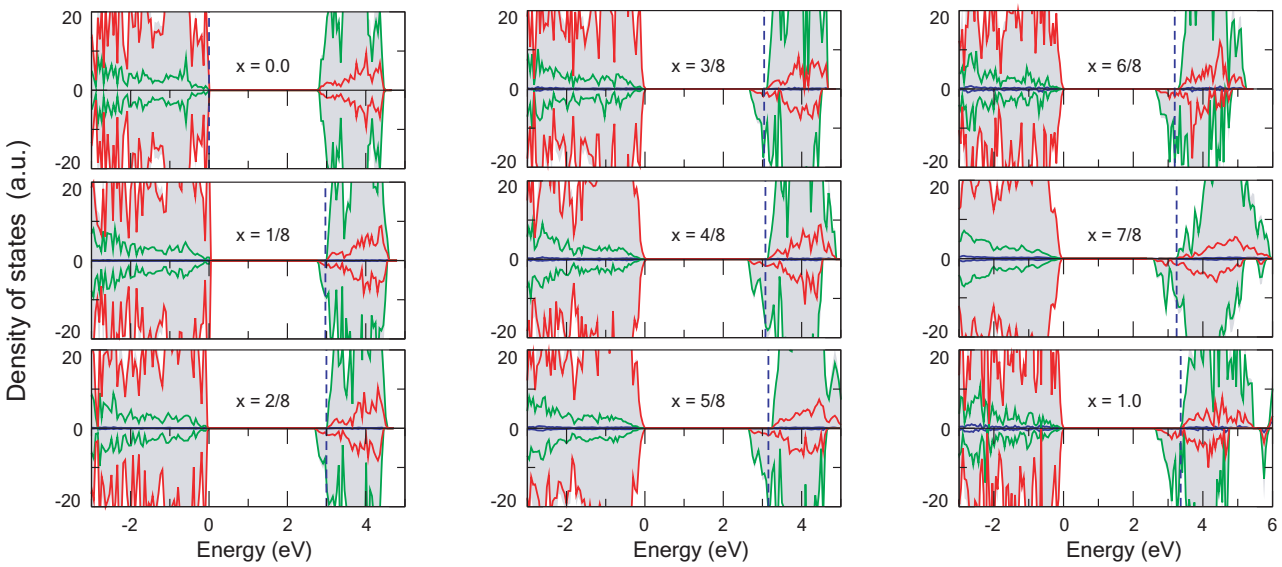

Figure S4. Atom resolved partial DOS (PDOS) of $Na_xTi_2O_4$ in the double phase.

Here, the solid lines in red, green and blue color represent the PDOS for O-2*p*, Ti-3*d* and Na-2*s* states, respectively. The gray-colored background displays the total DOS (TDOS). The dashed lines in blue line indicate the Fermi levels. The upper and lower parts are for spin-up and spin-down states.

Li insertion properties

Table S4. Lattice constants (a, b, c) and unit cell volume (V) of $Li_yNa_xTi_2O_4$ (y = 0.0 ~ 0.75, x = 0.25 and 0.5) compounds with tunnel structure, namely LNTO-single and LNTO-double.

Li content	LNTO-single				LNTO-double			
	Lattice constants (Å)			Volume	Lattice constants (Å)			Volume
	a	b	c	(Å^3)	a	b	c	(Å^3)
Insertion into $Na_{0.25}Ti_2O_4$								
0/8	9.092	10.771	5.951	582.804	9.855	10.953	5.971	644.539
1/8	9.108	10.796	5.925	582.564	9.909	10.839	5.958	639.876
2/8	9.119	10.810	5.911	582.639	9.960	10.740	5.945	635.876
3/8	9.146	10.836	5.893	584.086	10.048	10.641	5.936	634.718
4/8	9.169	10.869	5.877	585.617	9.993	10.647	5.934	631.365
5/8	9.197	10.907	5.858	587.646	10.065	10.554	5.924	629.202
6/8	9.217	10.951	5.836	589.024	10.013	10.546	5.912	624.287
Insertion into $Na_{0.5}Ti_2O_4$								
0/8	9.174	10.795	5.934	587.625	9.673	11.230	5.934	644.627
1/8	9.202	10.820	5.914	588.834	9.788	11.074	5.932	642.931
2/8	9.234	10.851	5.895	590.604	9.873	10.953	5.925	640.734
3/8	9.261	10.878	5.870	591.281	9.902	10.862	5.928	637.282
4/8	9.288	10.911	5.846	592.485	9.923	10.854	5.921	637.681

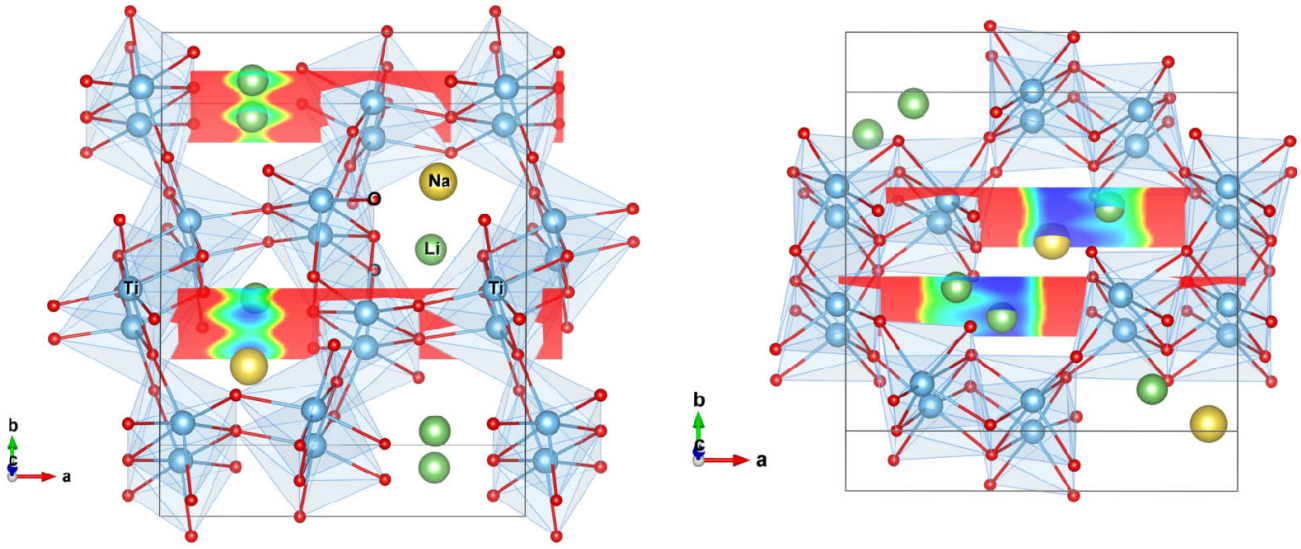

(a) LNTO-single (b) LNTO-double

Figure S5. The polyhedral view of the optimized crystal structure of Li inserted $Li_{0.75}Na_{0.25}Ti_2O_4$ compounds, namely (a) LNTO-single and (b) LNTO-double. The yellow and green balls illustrate Na and Li, respectively, and the color planes display the BVS map for Li atoms, where blue-to-green-to-yellow colors represent the ΔBVS increasing from 0.0 to 2.0, and red-colored area is responsible for restricted region with ΔBVS > 2.

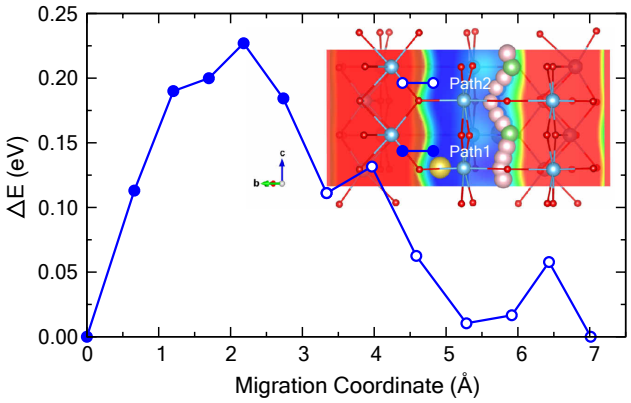

Figure S6. Energy profile caculated by NEB method for Li^+ ion migration along the *c*-axis in $Li_{0.125}Na_{0.25}Ti_2O_4$ (LNTO-double). The inset picture illustrates the Li^+ ion migration path inside the tunnel, along with the BVS map for Li.